ELSEVIER

Journal of Wind Engineering
and Industrial Aerodynamics 77&78 (1998) 591–602

JOURNAL OF wind engineering AND industrial aerodynamics

Discrete vortex simulation of flow around five generic bridge deck sections

Allan Larsen[a,*], Jens H. Walther[b]

[a] *COWI Consulting Engineers and Planners A/S, Parallelvej 15, DK-2800 Lyngby, Denmark*
[b] *Danish Maritime Institute, Hjortekoersvej 99, DK-2800 Lyngby, Denmark*

Abstract

Two-dimensional viscous incompressible flow past five generic bridge deck cross sections are investigated by means of the discrete vortex method. The analyses yields root mean square lift coefficients and Strouhal numbers for fixed cross sections and aerodynamic derivatives for the cross sections undergoing forced oscillatory cross wind and twisting motion. Fair agreement is established between the present simulations and wind tunnel test results reported in the literature.

Keywords: Computational bridge aerodynamics; Discrete vortex method; Vortex shedding; Aerodynamic derivatives

1. Introduction

Long span cable supported bridges are often found to be sensitive to wind effects, hence, wind loading and aeroelastic stability must be considered during design similarly to other loading components such as dead load, live load and possibly earthquake. Aerodynamic data for bridge design are traditionally obtained from wind tunnel tests, but the turn over time for planning, actual testing and analysis is often substantial and may be prohibitive for bridge design studies. In these cases the designer is forced to make use of aerodynamic data available in the literature but this approach involves large uncertainties.

A new computer code DVMFLOW based on the discrete vortex method has been developed in order to facilitate the acquisition of satisfactory aerodynamic data for use in bridge design studies without resorting to time consuming wind tunnel

* Corresponding author. E-mail: aln@cowi.dk.

0167-6105/98/$ – see front matter
PII: S0167-6105(98)00175-5

testing. The objective of DVMFLOW is to allow numerical assessment of aerodynamic parameters for practical 2D bluff cross-sections commonly encountered in design.

The present paper addresses the extraction of desired aerodynamic data from discrete vortex simulations and discusses their significance to aeroelastic analysis of bridges. Flow simulations and discussion of results will be given with reference to five generic bridge sections. These sections were investigated experimentally by Scanlan and Tomko [1] who reported aerodynamic derivatives for use in flutter analyses.

2. Discrete vortex code DVMFLOW

A distinct feature of flow past bluff bodies, stationary or in time dependent motion, is the shedding of vorticity in the wake which balances the change of fluid momentum along the body surface. Similar shedding of vorticity also occur in the wake of streamlined (airfoil like) bodies in transient motion in a potential flow. The vorticity shed at an instant in time is convected downstream but continues to affect the aerodynamic loads on the body.

Analytical treatment of potential flow past streamlined bodies assumes that the vortical wake is shed from a single point – the trailing edge. The shed vorticity is convected downwind with the speed of the surrounding fluid forming a trailing vortex sheet. This simplified model is not valid for viscous flows past stationary or moving bluff bodies. As a consequence of viscosity the unsteady vortical wake of a bluff body will be shed, not only at the trailing edge, but along the entire body contour. The shed vortices are convected down wind by local mean wind speed and viscous diffusion but will also interact to form large scale coherent structures. A mathematical model for the flow around bluff bodies was developed within the framework of the discrete vortex method as proposed by Turkiyyah et al. [2] for building aerodynamic problems. The present algorithm, which treats viscous diffusion by means of "random walks" as proposed by Chorin [3], was and programmed for computer by the co-author. The resulting numerical code DVMFLOW establishes a two-dimensional (2D) viscous and "grid free" time marching simulation of the vorticity equation well suited for computation of 2D bluff body flows. An outline of the mathematical model and the simulated flow about a flat plate is presented in Ref. [4]. Application to 4 selected bridge girder cross-sections and comparison to wind tunnel test results are discussed in Ref. [5].

The input to DVMFLOW simulations is a boundary panel model of the bluff body contour (the bridge deck section). The output of DVMFLOW simulations is time-progressions of surface pressures and section loads (drag, lift and moment). In addition, maps of the induced velocity field and vortex positions at prescribed time steps are available. Steady-state wind load coefficients are obtained from time averages of simulated loads on stationary panel models. Aerodynamic derivatives and vortex induced response are obtained from post processing of simulated time series of forced or free response.

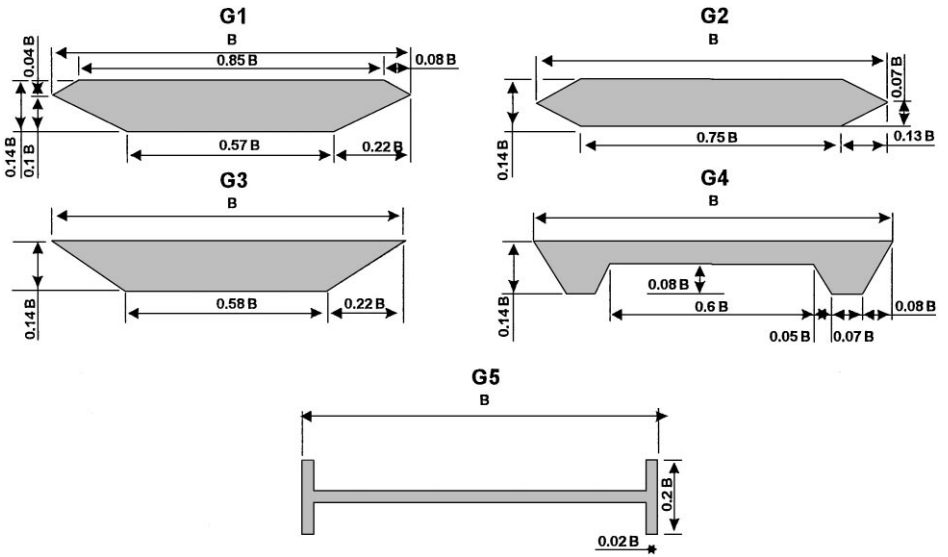

Fig. 1. Geometry of generic bridge girder cross-sections considered in the present study.

3. Five generic bridge deck cross-sections

Scanlan and Tomko [1] investigated a number of different bridge deck cross-section shapes in order to provide the bridge designer with experimental data for assessment of aerodynamic (flutter) stability. The present numerical study considers five of the generic sections tested by Scanlan and Tomko, four closed box sections and a 1:5 H-shaped cross-section similar to the plate girder of the 1st Tacoma Narrows bridge. The geometry of the individual sections investigated is shown in Fig. 1.

The circumference of each cross-section was subdivided into a total of 300 surface vortex panels. This discretisation allowed flow at Reynolds number $\mathrm{Re} = 10^5$ ($\mathrm{Re} = UB/v$) to be simulated.

3.1. Simulation of flow about stationary sections

A first step in the investigation was to simulate the flow and aerodynamic forces developing on the generic cross-sections fixed in space. An angle of attack of 0° of the wind flow was assumed (angle between flow direction and section chord). Each simulation was run for 30 non-dimensional time units $T = tU/B$ where t is the time, U the wind speed and B the cross-section width. A non-dimensional time increment $\Delta T = 0.025$ was adopted throughout the simulations.

At each time step the surface pressure distribution was computed from the local flux of surface vorticity. The section surface pressures were finally integrated along the contour to form time traces of aerodynamic section drag D, lift L and moment

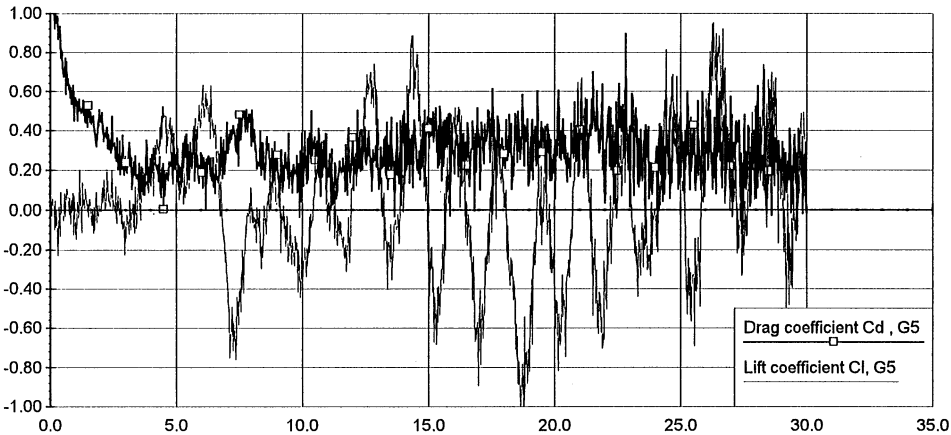

Fig. 2. Development of drag coefficient C_D and lift coefficient C_L for cross-section G5.

Fig. 3. Simulated von Kàrmàn vortex street developing in the wake of section G5. Flow visualisation by plotting the positions of vortex particles at a given instant in time.

M about mid-chord. Lastly, the computed aerodynamic forces were expressed in non-dimensional form using the conventional normalisation by dynamic head and chord

$$C_D = \frac{D}{\frac{1}{2}\rho U^2 B}, \quad C_L = \frac{L}{\frac{1}{2}\rho U^2 B}, \quad C_M = \frac{M}{\frac{1}{2}\rho U^2 B^2}. \tag{1}$$

Fig. 2 shows an example of the simulated time traces of C_D and C_L obtained for the G5 section (1st Tacoma Narrows). The C_D trace displays very high initial values of C_D associated with the instantaneous start up of the flow simulation. After an exponential decay the C_D trace settles around a mean value $C_D = 0.27$ after approximately 5 non-dimensional time units. The C_L trace develops very distinct oscillations with period $T \approx 2$ associated with formation of vortex roll up – the well known von Kàrmàn vortex street, Fig. 3, visualised by plotting of the spatial position of the individual vortex particles.

Table 1
Flow fields, C_D,C_L^{rms} and St for the generic bridge deck sections considered

Steady state load coefficients and flow field at time $tU/B = 10$	C_D	C_L^{rms}	St
 G1	0.08	0.07	0.17
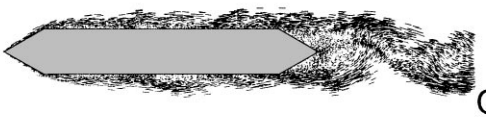 G2	0.08	0.08	0.17
 G3	0.10	0.08	0.10
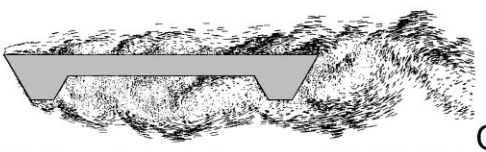 G4	0.08	0.12	0.17
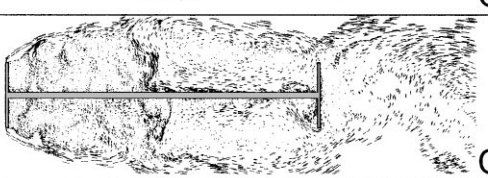 G5	0.27	0.33	0.11

A summary of flow patterns close to the sections and computed drag coefficients C_D, RMS lift coefficients C_L^{rms}, and Strouhal numbers St are given in Table 1. The Strouhal number quoted is based on cross wind section dimension H (depth), $St = fH/U$, in accordance with common practice.

From Table 1 it is noted that the closed box sections (sections G1, G2 and G3) displays better aerodynamic performance (lower C_D,C_L^{rms}) than the plate channel section G4. The H-shaped G5 section (1st Tacoma Narrows) appear to yield the worst aerodynamic performance.

3.2. Simulation of motion dependent aerodynamic forces

Motion dependent forces will develop when a bluff or streamlined body is set in time dependent motion in an otherwise steady fluid flow. These forces are responsible for the development of aerodynamic damping and possibly flutter instability at

sufficiently high flow speeds. Scanlan and Tomko [1] proposed a formulation of motion induced aerodynamic forces (L section lift, M section moment) suitable for two-dimensional cross-sections in cross wind bending and twisting motion. The original formulation involved 6 non-dimensional coefficients (the aerodynamic derivatives) to be derived from wind tunnel tests with elastically suspended section models. A logical extension of the original 6 coefficient formulation, proposed by Larsen [6], involves 8 aerodynamic derivatives:

$$L = \rho U^2 B\left[KH_1^*\frac{h'}{U} + KH_2^*\frac{B\alpha'}{U} + K^2H_3^*\alpha + K^2H_4^*\frac{h}{B}\right], \tag{2}$$

$$M = \rho U^2 B^2\left[KA_1^*\frac{h'}{U} + KA_2^*\frac{B\alpha'}{U} + K^2A_3^*\alpha + K^2A_4^*\frac{h}{B}\right]. \tag{3}$$

$K = \omega B/U$ is non-dimensional frequency, h, h' is the vertical cross wind motion and its time derivative and α, α' is the section rotation (twist) and corresponding time derivative. H_j^*, A_j^*, $j = 1, \ldots, 4$, are the aerodynamic derivatives which in general are functions of K.

Assuming that the section motions are harmonic in time $h = h\exp(\mathrm{i}\omega t)$, $\alpha = \alpha\exp(\mathrm{i}\omega t)$ (i being the time imaginary unit) and the aerodynamic process to be linear, the motion induced forces are also expected to be harmonic in time with identical frequency ω but phase shifted relative to the motion. Under these assumptions the above equations can be rearranged in non-dimensional form to yield:

$$C_L e^{\mathrm{i}(\omega t-\varphi)} = 2K^2\left[(\mathrm{i}H_1^* + H_4^*)\frac{h}{B} + (\mathrm{i}H_2^* + H_3^*)\alpha\right]e^{\mathrm{i}\omega t}, \tag{4}$$

$$C_M e^{\mathrm{i}(\omega t-\varphi)} = 2K^2\left[(\mathrm{i}A_1^* + A_4^*)\frac{h}{B} + (\mathrm{i}A_2^* + A_3^*)\alpha\right]e^{\mathrm{i}\omega t}. \tag{5}$$

Dividing the above equations by $\exp(\mathrm{i}\omega t)$, substituting $\exp(-\mathrm{i}\varphi)$ by $(\cos\varphi - \mathrm{i}\sin\varphi)$ and rearranging yields the following set of identities for determining the aerodynamic derivatives:

$$\left(\frac{U}{fB}\right)^2\frac{C_L(\cos\varphi - \mathrm{i}\sin\varphi)}{2(2\pi)^2 h/B} = \mathrm{i}H_1^* + H_4^*, \tag{6}$$

$$\left(\frac{U}{fB}\right)^2\frac{C_L\ (\cos\varphi - \mathrm{i}\sin\varphi)}{2(2\pi)^2\alpha} = \mathrm{i}H_2^* + H_3^*, \tag{7}$$

$$\left(\frac{U}{fB}\right)^2\frac{C_M(\cos\varphi - \mathrm{i}\sin\varphi)}{2(2\pi)^2 h/B} = \mathrm{i}A_1^* + A_4^*, \tag{8}$$

$$\left(\frac{U}{fB}\right)^2\frac{C_M(\cos\varphi - \mathrm{i}\sin\varphi)}{2(2\pi)^2\alpha} = \mathrm{i}A_2^* + A_3^*. \tag{9}$$

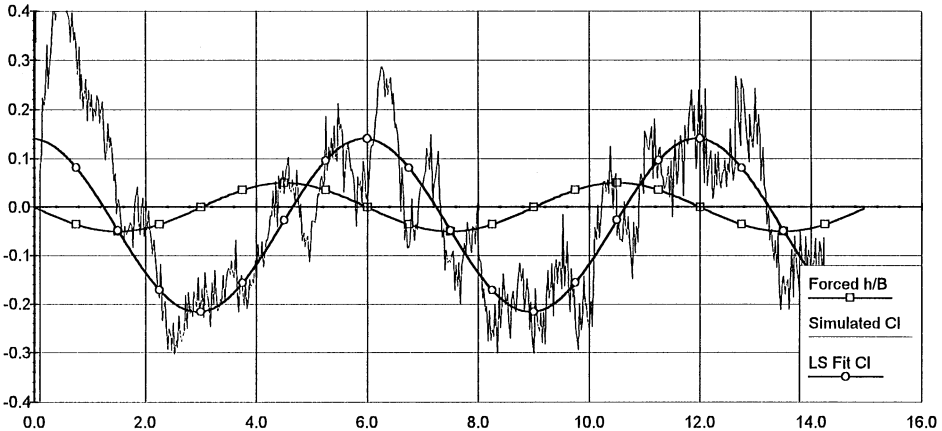

Fig. 4. Forced non-dimensional vertical bending h/B, simulated C_L time-trace and corresponding least-squares fit at $U/fB = 6$ obtained for the G1 cross-section.

The above formulation suggests the following procedure for extraction of the aerodynamic derivatives from methods capable of determining section forces, i.e. discrete vortex simulations:

(1) Impose a forced harmonic motion in vertical bending (h) or twist (α) on the cross-section contour to be investigated and carry out the discrete vortex simulations. (2) Extract the amplitude C_L,C_M of the induced non-dimensional lift and moment at frequency equal to that of the imposed motion. (3) Determine the phase shift of the aerodynamic forces relative to the imposed motion and substitute in Eqs. (6)–(9) in order to calculate the desired aerodynamic derivatives.

3.3. Five generic cross-sections

Discrete vortex simulations were carried out for the five generic bridge deck cross-sections of Fig. 1 following the procedure outlined above. The simulations covered the reduced wind speed range $2 < U/fB < 12$ at increments of 2, i.e. a total of 12 simulation runs per section. Each individual simulation was run for a non-dimensional time corresponding to $2\frac{1}{2}$ periods of imposed motion. Bending simulations were carried out at a forced motion amplitude $h/B = 0.05$. Twist simulations were carried out at $\alpha = 3.0^\circ$. The analysis of the simulations involved a least-squares fitting of a sinusoid to the simulated C_L and C_M time traces. An example of this procedure is shown in Fig. 4 obtained for section G1 for $h/B = 0.05$ at $U/fB = 6$.

As an example the derivation of the H_1^* aerodynamic derivative, the coefficient proportional to the lift damping will be considered. The C_L amplitude and the phase angle φ (in radians) are obtained from Fig. 4 as follows:

$$C_L = 0.18, \quad \varphi = (1.75/6) \times 2\pi = 1.83 \text{ rad}.$$

Hence from Eq. (6)

$$H_1^* = -\left(\frac{U}{fB}\right)^2 \frac{C_L \sin\varphi}{2(2\pi)^2 h/B} = -6^2 \frac{0.18 \sin(1.83)}{2(2\pi)^2 \times 0.05} = -1.585.$$

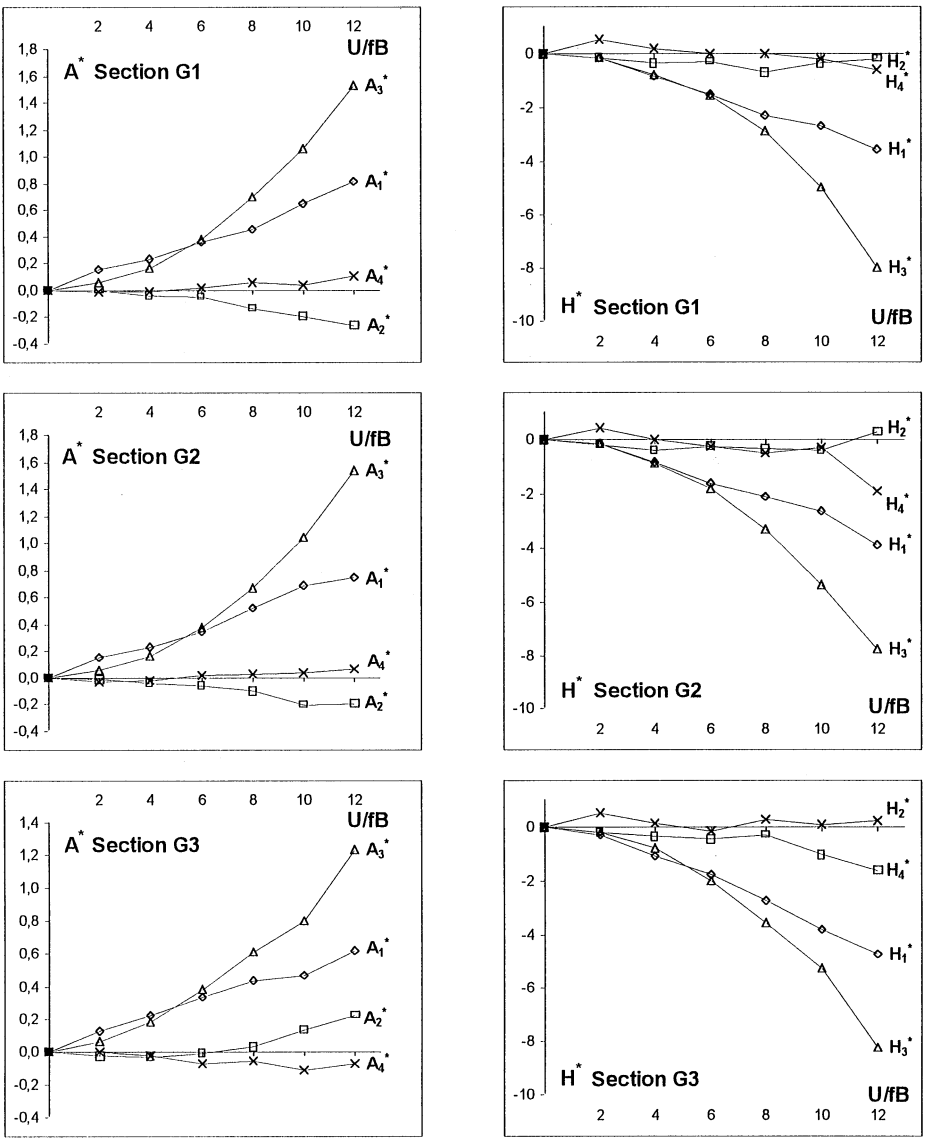

Fig. 5. Aerodynamic derivatives obtained from discrete vortex simulations of the flow about the generic sections G1, G2, G3, G4 and G5 in forced oscillatory motion.

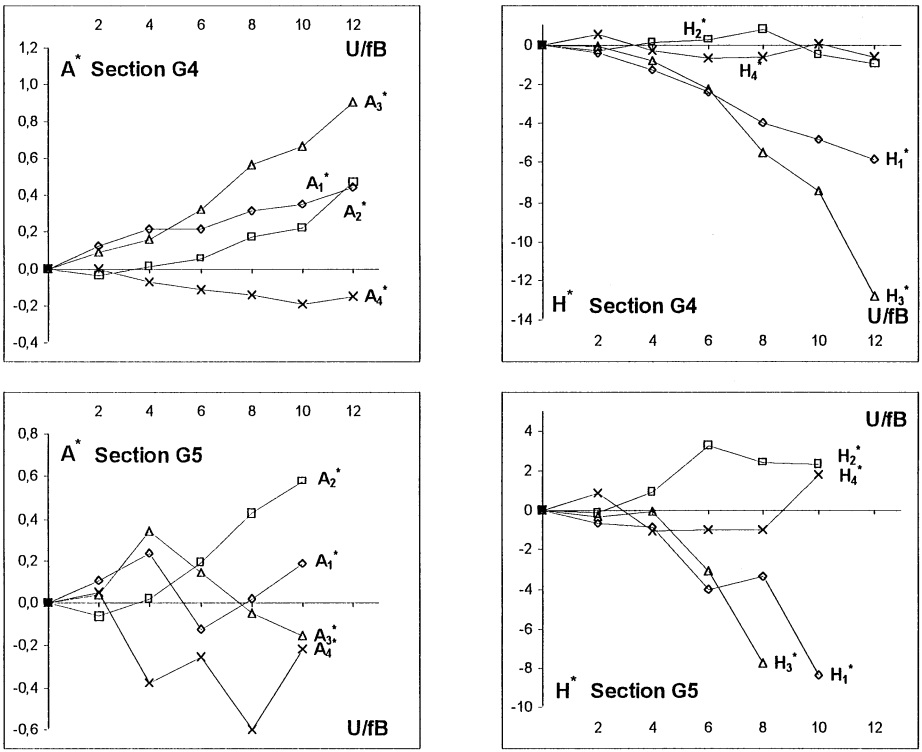

Fig. 5. Continued.

The extraction procedure illustrated above has been automated for computer using correlation techniques well established in signal analysis. This routine runs automatically once the starting point in time is specified for the analysis.

Aerodynamic derivatives obtained for the five generic sections considered are shown in graphic form in Fig. 5.

3.4. Comparison to experiments

A few comments on the aerodynamic derivatives obtained from the discrete vortex simulations and a comparison to experimental data are appropriate. Fig. 6 compares simulated derivatives for box sections G1 and G2 to experimental data presented in Ref. [1]. All simulated aerodynamic derivatives compare very well to the airfoil data (A) except for A_2^* which assumes numerical values about half those of the airfoil. The comparison between simulated and measured aerodynamic derivatives is quite reasonable except for H_2^*, for which the experimental data assumes opposite polarity and substantially higher numerical values. The A_2^* derivative remains negative at all wind speeds considered yielding coupled two-degree-of-freedom flutter for the G1 and G2 sections.

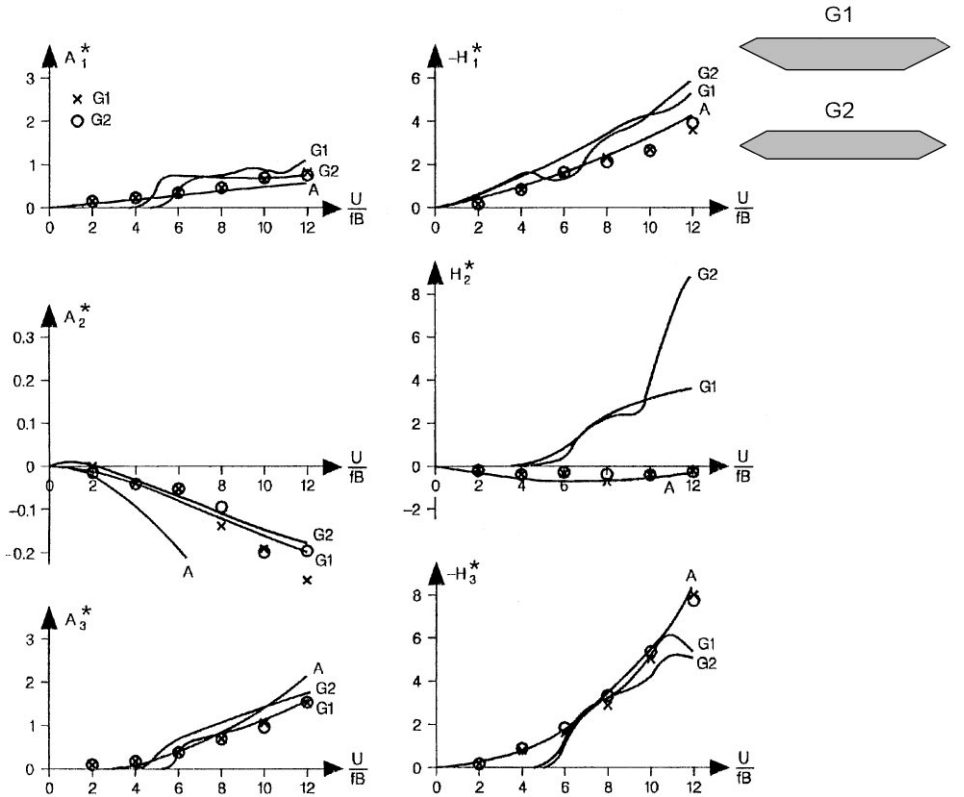

Fig. 6. Comparison of aerodynamic derivatives obtained from discrete vortex simulations to aerodynamic derivatives obtained from wind tunnel tests. Sections G1 and G2.

Fig. 7 compares simulated derivatives for the box, channel and plate sections G3, G4 and G5 to wind tunnel data. The comparison is in general less convincing than for sections G1 and G2 except for the H_3^* derivative for which simulations and measurements are in good agreement. The important aeroelastic feature of the G3, G4 and G5 sections is the cross over of the A_2^* derivative from negative values at low U/fB to positive values at higher U/fB. This behaviour indicates the onset of one-degree-of-freedom flutter at the reduced wind speed for cross over. Based on discrete vortex simualtions onset of flutter for section G3 is expected at $U/fB \approx 7.5$ as opposed to $U/fB \approx 8.5$ when judged from experiments. Sections G4 and G5 appear to be less aerodynamically stable yielding the onset of flutter at $U/fB \approx 4$ when judged from simulations. The experimental data yields the onset of flutter at $U/fB \approx 5$ for section G3 and at $U/fB \approx 2$ for section G5.

The discrepancies noted between simulated and measured aerodynamic derivatives cannot be resolved at present but two plausible causes shall be noted. Simulated aerodynamic derivatives were derived directly from motion induced forces whereas

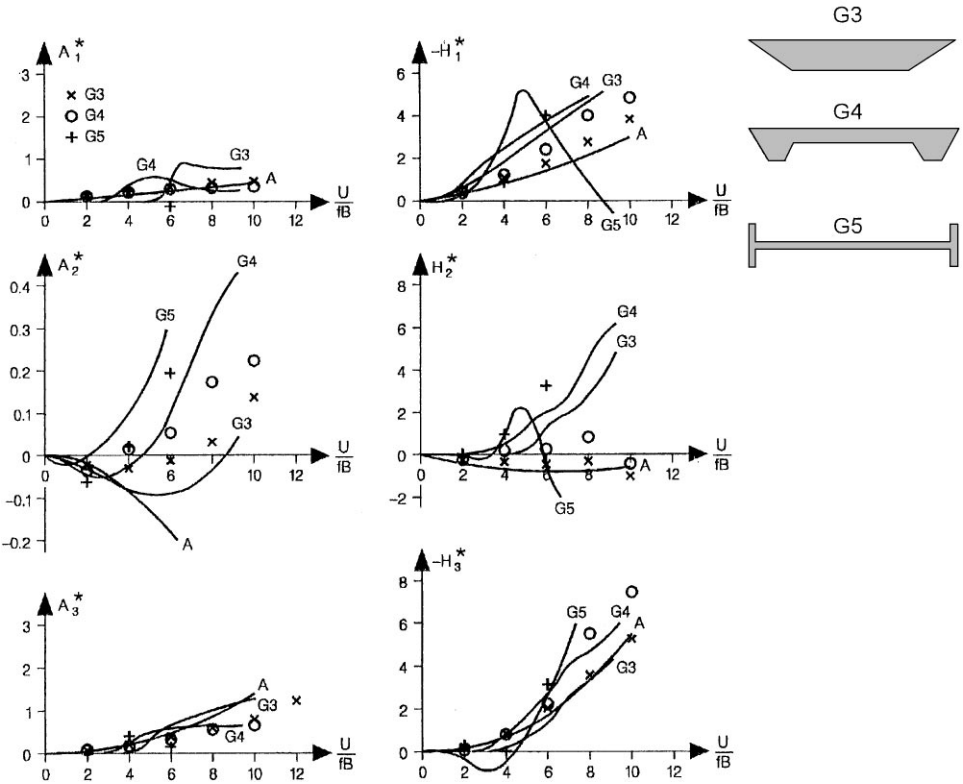

Fig. 7. Comparison of aerodynamic derivatives obtained from discrete vortex simulations to aerodynamic derivatives obtained from wind tunnel tests. Sections G3, G4 and G5.

the wind tunnel data was obtained from analysis of free response measurements fitted to the original 6 coefficient formulation [1]. The latter process may have linked A_4^* and H_4^* effects to the remaining derivatives. Another important aspect is a possible non-linear effect of motion amplitude which, in particular, is expected to influence sections displaying one-degree-of-freedom torsion flutter. Twist amplitudes imposed in the wind tunnel tests are unknown.

4. Conclusion

The paper presents computerised discrete vortex simulations of the flow of five generic bridge deck sections stationary or in forced harmonic motion relative to the wind flow. Comparison of simulations to experimental data given in the literature displays fair to good agreement indicating that the present computational method may be an efficient tool in the design of new bridge deck cross-sections.

Acknowledgements

The present study was supported by the COWI foundation. Their keen interest in the development of bridge aerodynamics is highly appreciated. The authors also extend their appreciation to Mr. Harold Bosch of the Turner-Fairbank Highway Research Centre for providing information on the geometry of the generic cross-sections investigated.

References

[1] R. Scanlan, J.J. Tomko, Airfoil and bridge deck flutter derivatives, J. Mech. Div., EM6, Proc. ASCE, December 1971.
[2] G. Turkiyyah, D. Reed, J. Yang, Fast vortex methods for predicting wind-induced pressures on buildings, J. Wind Eng. Ind. Aerodyn. 58 (1995) 51–79.
[3] A.J. Chorin, Numerical study of slightly viscous flow, J. Fluid Mech. 57 (1973) 785–796.
[4] J.H. Walther, A. Larsen, 2D discrete vortex method for application to bluff body aerodynamics, J. Wind Eng. Ind. Aerodyn. 67&68 (1997) 183–193.
[5] A. Larsen, J.H. Walther, Aeroelastic analysis of bridge girder sections based on discrete vortex simulations, J. Wind Eng. Ind. Aerodyn. 67&68 (1997) 253–265.
[6] A. Larsen, Prediction of aeroelastic stability of suspension bridges during erection, J. Wind Eng. Ind. Aerodyn. 72 (1997) 265–274.